Uncovering Quantum Entanglement and Bell Nonlocality in $\tau^+\tau^-$ at the Large Hadron Collider through Machine Learning for Neutrino Reconstruction Baihong Zhou (TDLI)

In collaboration with Yulei Zhang², Qibin Liu¹, Matthew Low³, Tong Arthur

Wu³, Shu Li¹, Tao Han³, Shih-Chieh Hsu²

- 1. Tsung-Dau Lee Institute, SJTU;
- 2. University of Washington, Seattle;
- 3. University of Pittsburgh, Pittsburgh;

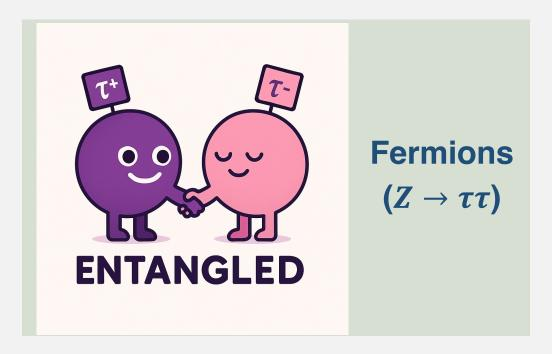
Link: 2504.01496



 Quantum entanglement is one of the hallmarks of quantum mechanics, which has been observed from the microscopic to the macroscopic, while it still remains to be further validated in the TeV scale;

Bosons $(H \rightarrow VV)$

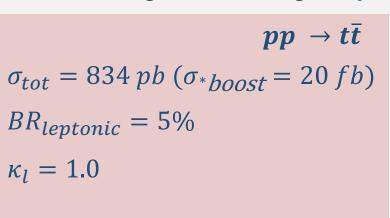






- In the ATLAS experiment, the Quantum Entanglement has been observed in the $pp \to t\bar{t}$ process;
- It remains comparatively **unexplored in the** $pp \rightarrow \tau \tau$ **system**, which

is worth taking a look using **Delphes**;



*boost:
$$m_{t\bar{t}} > 800 \; GeV$$

$$pp \rightarrow Z \rightarrow au au$$

$$\sigma_{tot} = 1848 \ pb$$

$$BR_{\pi} = 10\%$$

$$\kappa_{\pi} = 1.0$$

Pure, entanglement

With Z dominate:

$$\rho_{\tau\bar{\tau}} = \lambda \tilde{\rho}^{(+)} + (1 - \lambda) \tilde{\rho}_{mix}$$

$$(g_A^{\tau})^2 - (g_V^{\tau})^2$$

$$\lambda = \frac{(g_A)^{} - (g_V)^{}}{(g_A^{})^2 + (g_V^{})^2}$$

$$\rho = \frac{1}{4} \left(\mathbb{I}_2 \otimes \mathbb{I}_2 + \sum_i B_i^+ \sigma_i \otimes \mathbb{I}_2 + \sum_j B_j^- \mathbb{I}_2 \otimes \sigma_j + \sum_{ij} C_{ij} \sigma_i \otimes \sigma_j \right) [1]$$

[1] Pairs of two-level systems;

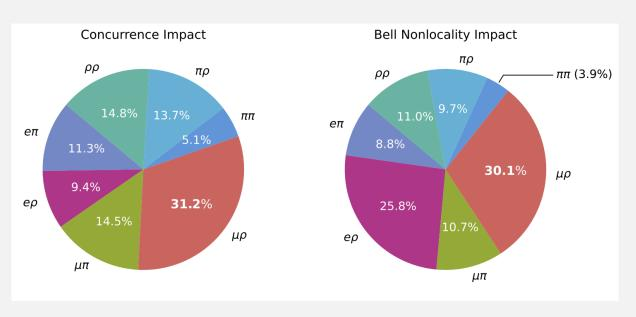
^[2] Constraining new physics in entangled two-qubit systems: top-quark, tau-lepton and photon pairs;



- In the $\tau\bar{\tau}$ system, the density matrix ρ consists of a **mixture** of pure entangled and separable states, thus placing stricter constraints on the τ reconstruction;
- 7 distinct ττ decay subchannels are taken into account for this analysis;

Decay	Spin Analyzing Power	Branching Ratio
$\pi \nu_{\tau}$	1.00	10.82%
$ ho(\pi\pi^0) u_ au$	0.41	25.52%
$e \nu \nu_{ au}$	-0.33	17.82%
$\mu u u_{ au}$	-0.34	17.39%

Single τ decay



Overall results benefits from all channels



• The $\tau \bar{\tau}$ system is **under constrains**, which means some **estimation techniques** are required;

$$\tau^{+}\tau^{-} \rightarrow \pi^{+}\pi^{-}$$

$$E_{x,y}^{miss} = p_{x,y}^{\nu_{1}} + p_{x,y}^{\nu_{2}} \quad \text{8 unknown,}$$

$$E_{\nu_{i}}^{2} - \overline{p_{\nu_{i}}}^{2} = 0 \quad \textbf{6 constrains}$$

$$m_{\tau_{i}}^{2} = (E_{\nu_{i}} + E_{\pi_{i}})^{2} - (\overline{p_{\nu_{i}}} + \overline{p_{\pi_{i}}})^{2}$$

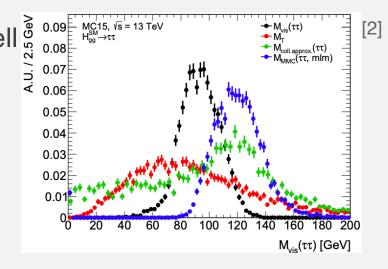
$$\tau^{+}\tau^{-} \to \ell^{+}\ell^{-}$$

$$E_{x,y}^{miss} = p_{x,y}^{\nu_{1}} + p_{x,y}^{\nu_{2}} \quad \text{8 unknown,}$$

$$\mathbf{4 constrains}$$

$$m_{\tau_{i}}^{2} = (E_{\nu_{i}} + E_{\pi_{i}})^{2} - (\overline{p_{\nu_{i}}} + \overline{p_{\pi_{i}}})^{2}$$

- Some techniques, like **Missing Mass Calculator** (MMC)^[1] has been well on the ATLAS experiments;
- In this study, we trained one **generative model** for ν reconstruction;



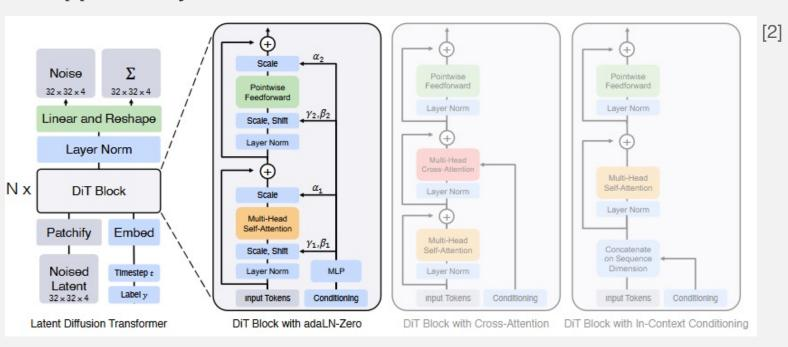
 $^{^{[1]}}$ A new mass reconstruction technique for resonances decaying to au au

^[2] Effects of tau decay product reconstruction in a Higgs CP analysis with the ATLAS experiment



- In many generation tasks, the diffusion models together with the Transformer framework have emerged at the forefront, indicating their strong potential in the ν reconstruction;
- The **Point-Edge Transformer (PET)** body and the **generation** head of *OmniLearn* ^[1] is a good way to indicate the three momenta of ν in our $pp \to \tau\tau$ system with the **diffusion model**;



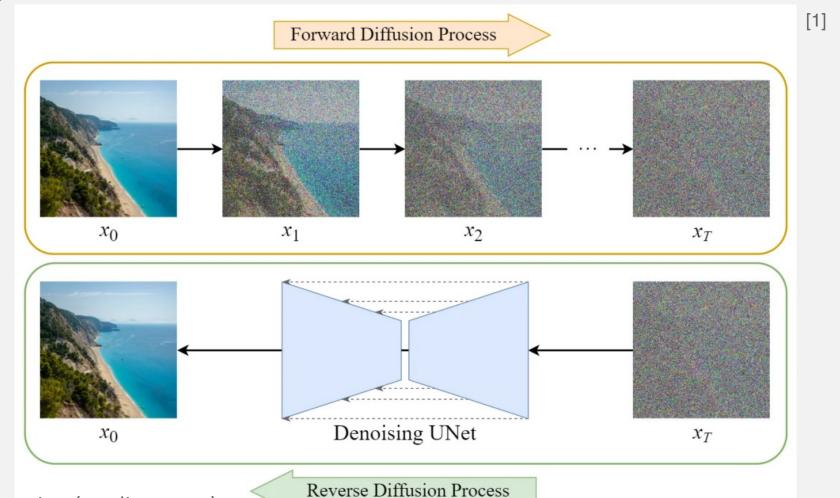


^[1] Solving Key Challenges in Collider Physics with Foundation Models

^[2] Scalable Diffusion Models with Transformers



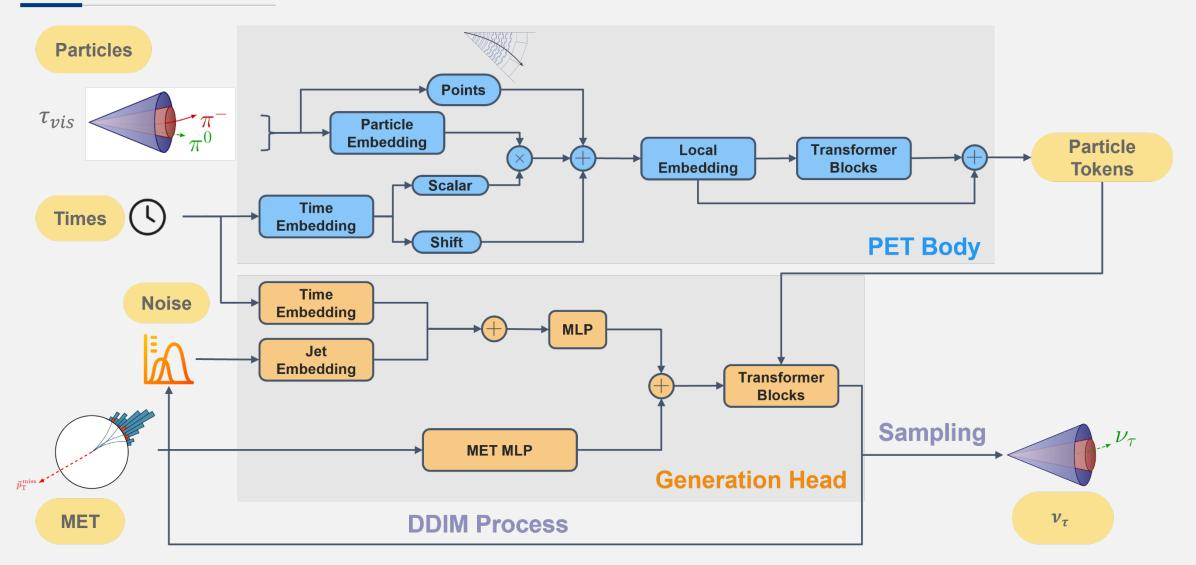
• Diffusion model is a **generative model** that adding noise in the training process and denoising in the evaluation process;



< 7 >

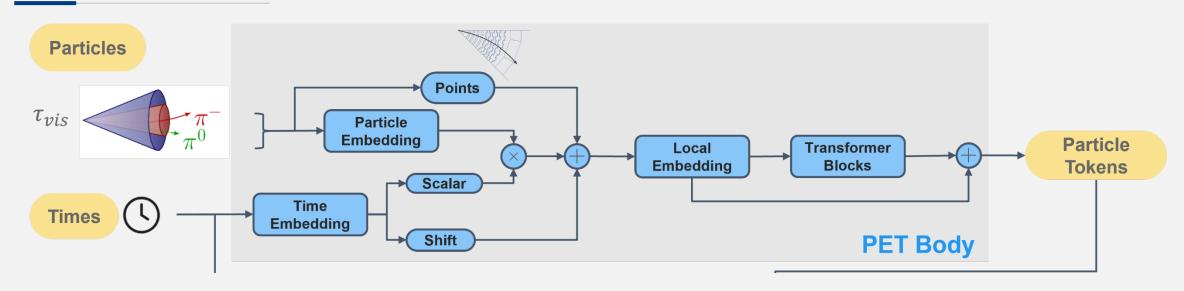
Architectures





Architectures – PET Body





PET Body: Tokens Generation Network

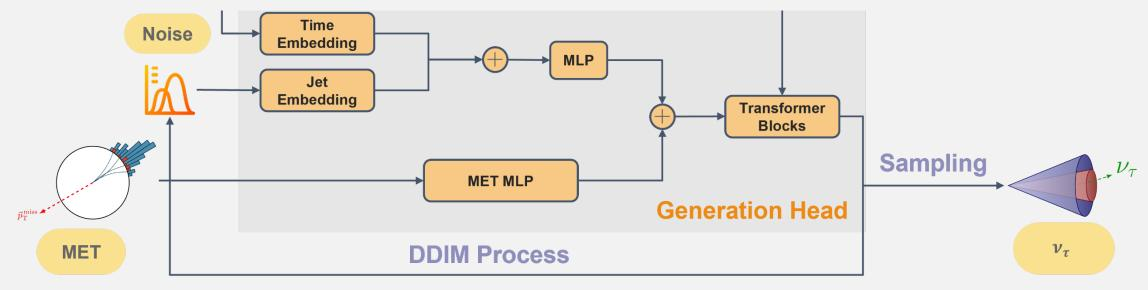
- **Points**: Represent the (η, ϕ) coordinates of the input particles;
- Edge features: Combine particle features and their neighbor differences;
- **Time**: Control the process of adding noise to the original distribution;
- Transformer Blocks: Capture and model the relationships between the input features;
- Output: the tokens that directs the generation head;

Architectures – Generation Head



Generation Head: Final Three-Momentum Generation of ν

- Particle tokens: Generated from the PET body;
- Time: Control the process of adding noise to the original distribution;
- MET: Guide the generation head towards the appropriate distribution;
- Sampling Process: Utilize Denoising Diffusion Implicit Models (DDIM)^[1] to produce the three-momentum of ν ;



Input variables



- 7 distinct ττ decay subchannels are trained separately using a consistent strategy for variable input, training and evaluation. All input variables are at the reconstruction level;
- To increase the number of training samples, the strategy of **randomly rotating** the system along the z-axis is used. Additionally, the τ constitutes are required the kinematics **remain consistent with** the original data.

Subchannel	Original number of samples	Number of samples after random boost
$\pi\pi$	304k	15.5M
$e\pi$	147k	14.8M
$\mu\pi$	193k	19.5M
πho	111k	10.9M
e ho	54k	0.600M
μho	73k	0.817M
ho ho	38k	3.72M

Input variables



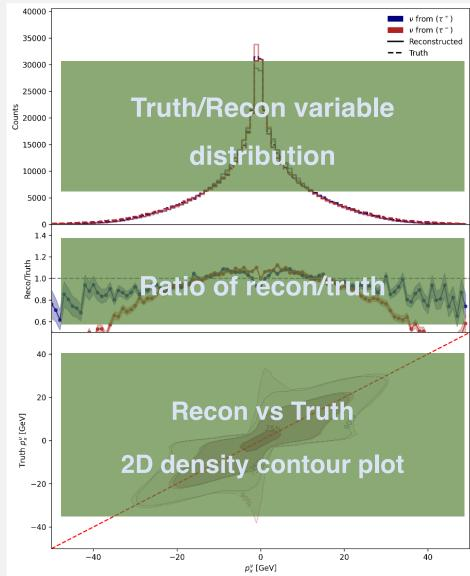
- 7 distinct ττ decay subchannels are trained separately using a consistent strategy for variable input, training and evaluation. All input variables are at the reconstruction level;
- To increase the number of training samples, the strategy of **randomly rotating** the system along the z-axis is used.
- The input variables are listed in the table below:

Category	Variables	Description
$E_T^{ m miss}$	$(p_T^{ m miss},\phi^{ m miss})$	Missing transverse momentum vector
au Visible Components	(p_T, η, ϕ, E) Charge PID	Four-momentum Electric charge of τ -visible parts Electron, muon, or pion identification
Small-R Jets	(p_T, η, ϕ, E) Charge PID	Four-momentum Electric charge of the jet Particle identification

Neutrino Reconstruction

- **Purpose**: Precisely reconstruct ν to reconstruct τ with high precision.
- Methods: Use Diffusion model to reconstruct ν with DDIM sampling methods.
- Evaluation: In the validation dataset (same amount of training dataset but not used in training), each event would generate 10 candidates.

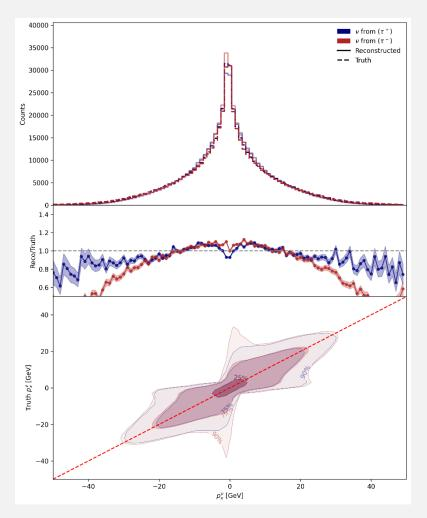


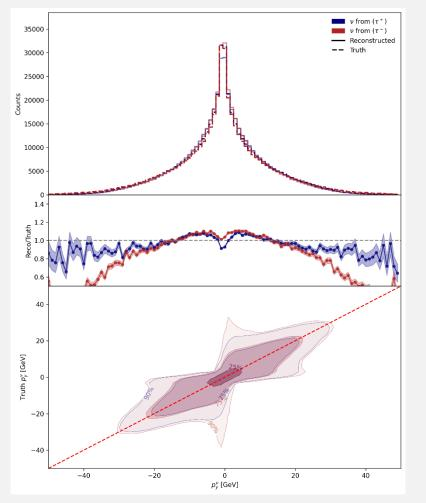


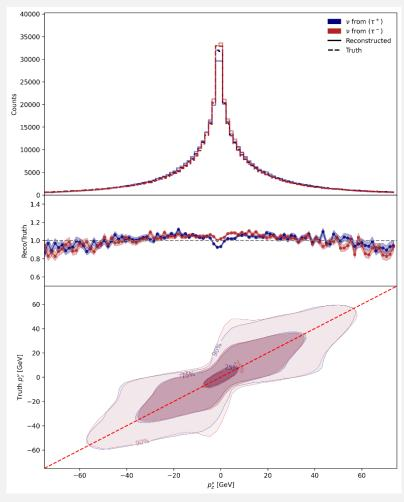
• Neutrino Reconstruction - $\pi\pi$



• Excellent reconstruction results have been achieved for the three-momentum of ν .



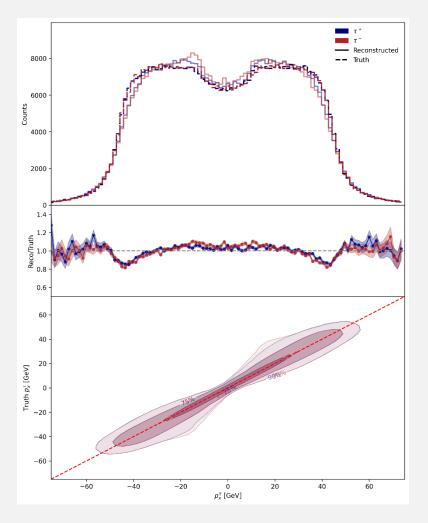


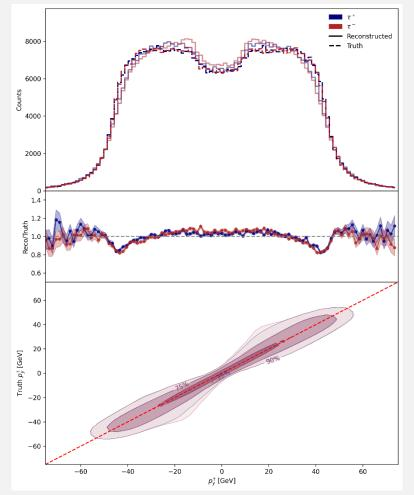


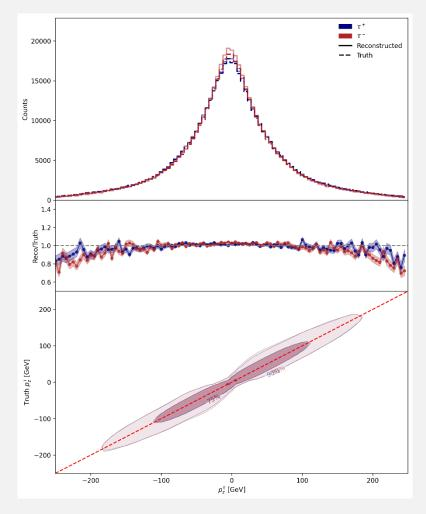
• Neutrino Reconstruction - $\pi\pi$



• Excellent reconstruction results have been achieved for the three-momentum of τ .



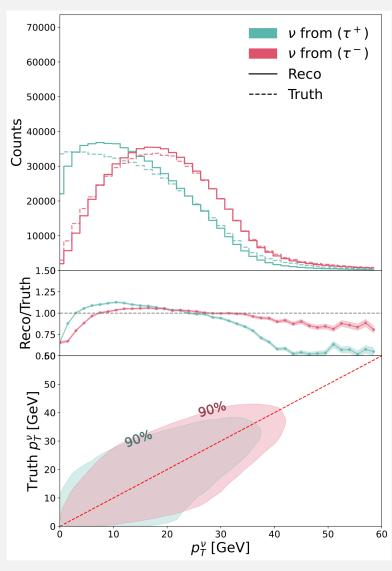




Neutrino Reconstruction - Comparison

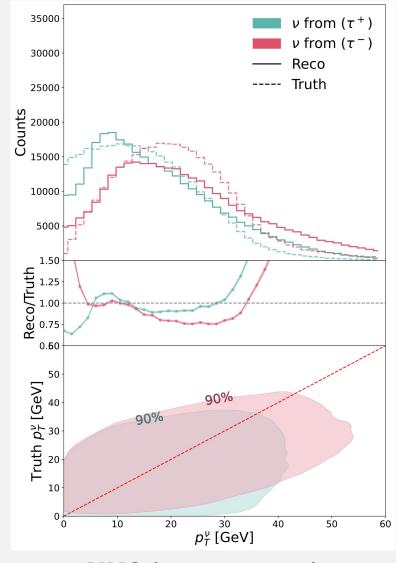
	$e\rho$	(%)	μρ	(%)
	ML	MMC	ML	MMC
$\Delta p_{\tau^+}^x$	15.72	26.72	16.03	26.62
$\Delta p_{\tau^+}^y$	15.50	26.00	16.04	27.83
$\Delta p^z_{\tau^+}$	15.70	25.65	16.12	26.69
$\Delta p_{\tau^-}^x$	15.69	26.47	16.02	26.85
$\Delta p_{\tau^-}^y$	15.34	26.87	16.15	27.39
$\Delta p^z_{\tau^-}$	15.81	26.26	16.26	25.67
$\Delta m_{ au au}$	5.81	22.70	5.76	22.81

Half-Width at Half-Maximum (HWHM)



Diffusion $(l\rho-channel)$





 $\mathsf{MMC}\left(l\rho-channel\right)$

Neutrino Reconstruction - 7 subchannels



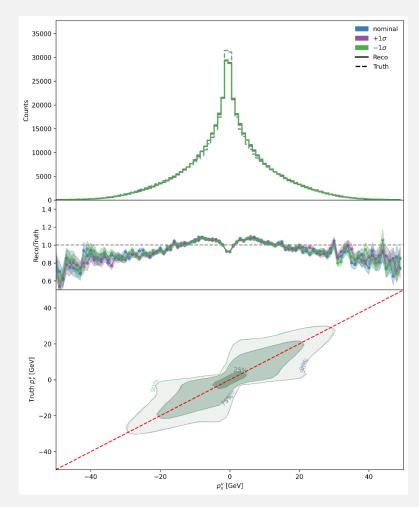
• To quantify the resolution of the reconstructed distributions, the **HWHM** is used as a metric.

	$\pi\pi$	(%)	$e\pi$	(%)	$\mu\pi$	(%)	$\pi \rho$	(%)	$e\rho$	(%)	μρ	(%)	ρρ	(%)	
	ML	MMC	ML	MMC	ML	MMC	ML	MMC	ML	MMC	ML	MMC	ML	MMC	
$\Delta p_{\tau^+}^x$	18.97	25.99	18.34	27.91	19.30	28.56	16.19	25.45	15.72	26.72	16.03	26.62	16.38	25.65	
$\Delta p_{\tau^+}^y$	19.01	26.02	18.54	27.26	19.33	28.15	15.96	25.26	15.50	26.00	16.04	27.83	16.38	25.28	71 %
$\Delta p_{ au^+}^z$	19.47	25.48	19.52	27.46	20.00	27.19	16.31	24.85	15.70	25.65	16.12	26.69	16.49	25.02	improvements
$\Delta p_{ au^-}^x$	18.77	25.78	17.06	28.38	17.69	27.43	18.11	26.13	15.69	26.47	16.02	26.85	16.34	25.17	
$\Delta p_{ au^-}^y$	18.71	25.96	16.62	26.22	17.33	28.13	17.89	25.79	15.34	26.87	16.15	27.39	16.36	25.40	
$\Delta p^z_{\tau^-}$	19.69	25.43	17.06	26.27	17.75	27.17	18.44	25.49	15.81	26.26	16.26	25.67	16.72	24.23	057.9/
$\Delta m_{ au au}$	7.94	23.27	6.18	24.91	6.41	24.31	7.24	22.72	5.81	22.70	5.76	22.81	6.27	21.89	257 % improvements

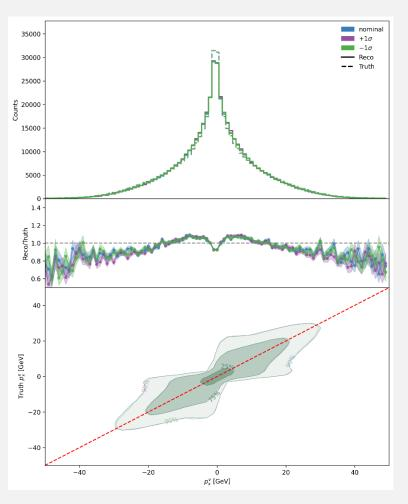
Neutrino Reconstruction - Systematics



• The **network's robustness** is evaluated by: [1]



Perturbing the **MET** information by ± 1 *GeV*

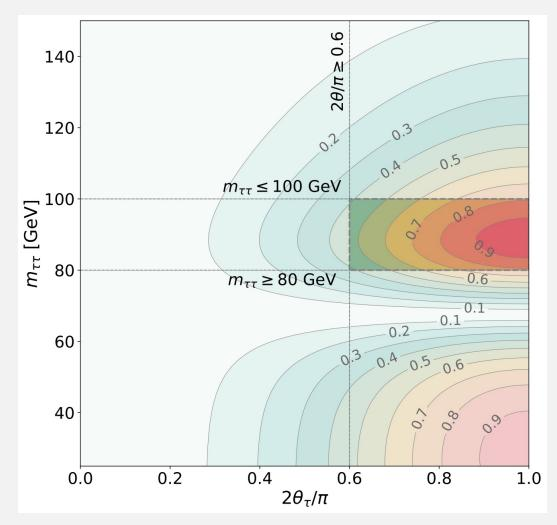


Applying a 3% shift to all input variables

Signal Region Definition



Signal Region (with triggers)



9.0 140 2θ/π≥ 120 $m_{\tau\tau} \leq 100 \text{ GeV}$ m₁₇ [GeV] $m_{\tau\tau} \ge 80 \text{ GeV}$ 0.0 -0.3-0.4-0.260 0.1 0.2 40 0.0 0.2 0.4 0.6 8.0 1.0 $2\theta_{ au}/\pi$

Cocurrence (C > 0)

Bell Nonlocality (B > 0)

Signal Region Yields



Subchannel	Prongness	$ \kappa_A imes \kappa_B $	$ au au o\ell\pi$	$ au au o\ell ho$	$\tau \tau \to \pi \pi$	$ au au o\pi ho$	au au o ho ho
		SR &	$di-\tau$ Trigger (p)	$T_{T} > 35 \text{ GeV } \& p_{T}^{7}$	$T_T^2 > 25 \text{ GeV}$)		
$\pi\pi$			3.92 ± 0.18	0.09 ± 0.04	89.43 ± 0.48	2.90 ± 0.13	0.14 ± 0.04
πho			0.12 ± 0.03	22.71 ± 0.65	1.61 ± 0.06	206.39 ± 1.09	6.29 ± 0.28
$\rho\rho$			< 0.01	0.56 ± 0.10	0.06 ± 0.01	4.51 ± 0.16	629.99 ± 2.83
	SR & $e+\tau$ Trigger ($p_T^e>14$ GeV & $p_T^\tau>25$ GeV) or single- e Trigger ($p_T^e>26$ GeV)						
$e\pi$			378.90 ± 1.79	17.52 ± 0.57	< 0.01	0.01 ± 0.01	< 0.01
$e\rho$			8.33 ± 0.27	1233.90 ± 4.82	< 0.01	0.03 ± 0.01	0.15 ± 0.04
SR & $\mu + \tau$ Trigger $(p_T^\mu > 17~{\rm GeV}~\&~p_T^ au > 25~{\rm GeV}$) or single- μ Trigger $(p_T^\mu > 26~{\rm GeV})$							
$\mu\pi$			565.94 ± 2.19	25.21 ± 0.69	< 0.01	< 0.01	< 0.01
$\mu \rho$			12.63 ± 0.33	1862.06 ± 5.92	< 0.01	< 0.01	0.04 ± 0.02

Sig yields					
(Total: 4996.61±8.70)					
(per 1 fb^{-1})					

Subchannel	$W o \ell u$	W o au u	$Z \to \ell \ell$	$t \overline{t}$	QCD	Total		
	SR & di- $ au$ Trigger ($p_T^{ au_1} > 35~{ m GeV}$ & $p_T^{ au_2} > 25~{ m GeV}$)							
$\pi\pi$	< 0.01	< 0.01	< 0.01	< 0.01	< 0.01	< 0.01		
πho	< 0.01	< 0.01	< 0.01	0.05 ± 0.05	< 0.01	0.05 ± 0.05		
ho ho	< 0.01	< 0.01	< 0.01	0.10 ± 0.07	< 0.01	0.10 ± 0.07		
SR & e +	$ au$ Trigger (p_T^e)	> 14 GeV & p	$\sigma_T^{ au} > 25 \mathrm{GeV}$) or single- e Tri	$gger(p_T^e)$	26 GeV)		
$e\pi$	< 0.01	< 0.01	< 0.01	2.87 ± 0.38	< 0.01	2.87 ± 0.38		
e ho	1.93 ± 0.86	0.62 ± 0.36	< 0.01	11.19 ± 0.75	< 0.01	13.74 ± 1.20		
SR & μ +	$ au$ Trigger (p_T^{μ})	> 17 GeV & p	$\sigma_T^{ au} > 25 \mathrm{GeV}$) or single- μ Tr	igger (p_T^μ)	> 26 GeV)		
$\mu\pi$	< 0.01	0.41 ± 0.29	< 0.01	4.13 ± 0.46	< 0.01	4.55 ± 0.54		
$\mu \rho$	1.16 ± 0.67	0.62 ± 0.36	< 0.01	< 0.01	< 0.01	1.78 ± 0.76		

Bkg yields (Total: 23.10 \pm 1.57) (per 1 fb^{-1})



[1]

Decay Approach

- Measure the angle between τ and τ visible component in the τ rest frame;
- Use **template fit** to extract C_{ij} components;
 - $C_{ij} = \frac{9}{\kappa_a \kappa_b} < \cos \theta_i^a \cos \theta_j^b >$

Kinematic Approach

- **Parameterize** spin correlation matrix by θ (scattering angular) and β (speed of τ);
- Measuer the θ to get the C_{ij} ;

•
$$C_{ij} \approx \begin{pmatrix} 1 & 0 & 0 \\ 0 & \frac{\sin^2 \theta}{1 + \cos^2 \theta} & 0 \\ 0 & 0 & -\frac{\sin^2 \theta}{1 + \cos^2 \theta} \end{pmatrix}$$

Systematics

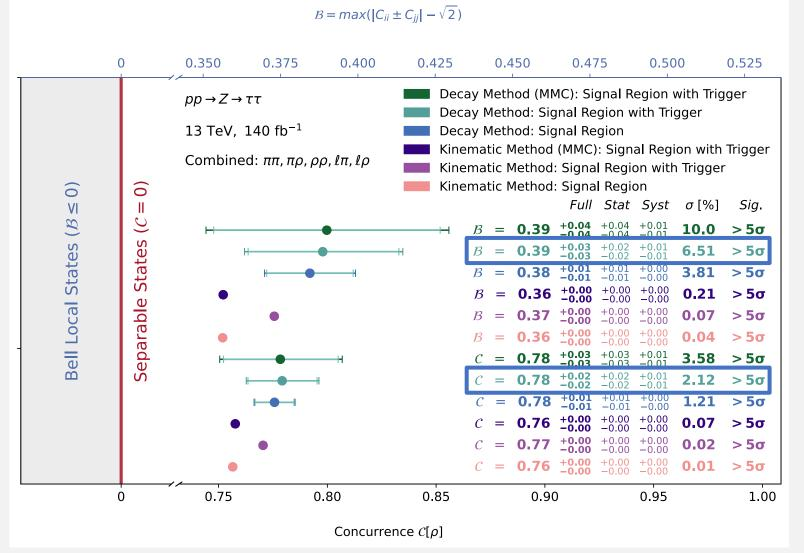


	SR Only SR & Trigger	Systematic Ir	mpact: $I_n = \sigma_{\text{total}}^{poi}$	$C_{poi,n}\sigma^n$				
_	31.28%	32.22%	31.00%	31.52%	31.87%	30.55% —	29.82%	31.35 %
—	33.04% —	33.37% —	29.81% —	30.73% —	30.27% —	30.22% —	29.76% —	31.29%
							А	II Systematics
-	28.40% —	29.58% —	28.93% —	29.92% —	29.64% —	30.08% —	29.55%	28.66%
-	29.58% —	31.79% —	29.31%—	29.72% —	29.67% —	30.00% —	29.56% —	30.05%
								MC Statistics
4	5.95% ◄	8.05% ◄	7.73%	2.80%	4.91%1	0.78%ı	0.74%	6.10%
	1.56%1	1.25%i	0.12%	0.67%ı	0.64%ı	0.07%i	0.08%ı	0.90%
								Luminosity
	< 0.01%	1.99%ı	1.51%	3.93%	3.53%ı	0.41%	0.05%1	1.06%
	1.33%ı	1.30%	3.39%	2.16%	2.48%ı	0.30%i	0.07%	2.01%
							Background	Cross-Section
	2.38%	2.97%	3.12%ı	1.03%	1.89%ı	0.26%ı	0.52%	2.41%
	1.57%	3.59%ı	0.23%ı	0.41%ı	0.47%ı	0.13%i	0.23%1	1.71%
							Signal	Cross-Section
	0.91%ı	1.17%ı	1.20%	5.18% -	5.49%ı	1.07%ı	0.89%ı	1.47%
ı	2.44%	2.59%1	1.47%	1.72%ı	1.61%	2.23%	2.50%	2.12%
							Tau	Energy Scale
4	8.81%	5.53%	2.41%	5.03%	3.26%	2.57%1	1.72% ◄	8.05%
4	9.21%	4.38%1	1.67%	2.92%	2.61%	2.03%1	1.50%	4.49%
							Je	et Enery Scale
4	7.25% -	7.32% ◀	6.68%	4.71% ◄	7.52% •	4.44%	3.42% ◄	7.11%
4	10.93% ◄	7.83%	3.66% ◀	6.67% ▮	4.45%	2.13%	1.90% ◀	6.57%
							So	ft MET (p_x, p_y)
	0.08%ı	0.04%ı	0.06%ı	0.05%i	0.02%ı	0.03%i	0.03%i	0.07%
	0.03%ı	0.01%i	0.02%ı	0.06%	0.02%ı	0.02%	0.02%i	0.03%
								ν Sampling
	ππ	πρ	ρρ	еπ	μπ	ер	μρ	Combined

Results



• By using ML methods to reconstruct ν , good results have been obtained;



Compare with MMC

54 %

improvements

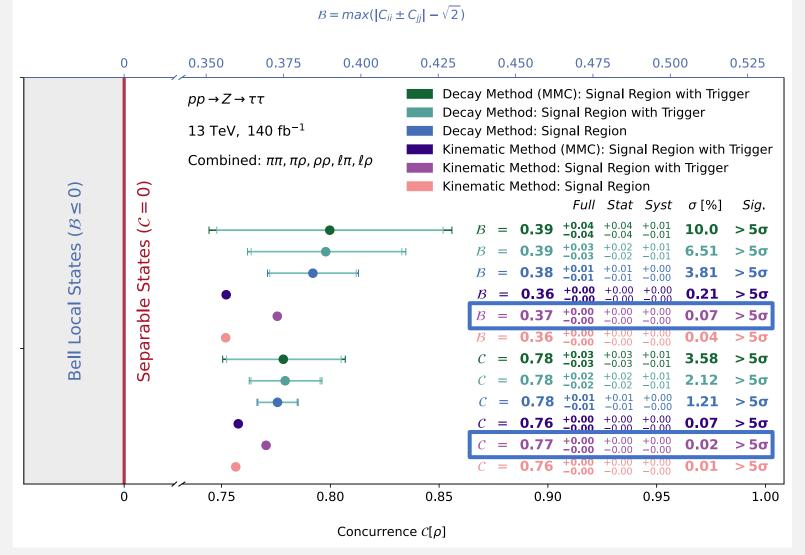
69 %

improvements

Results



• By using ML methods to reconstruct ν , good results have been obtained;



Compare with MMC

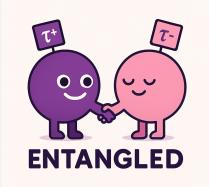
200 % improvements

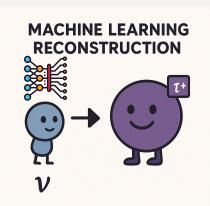
250 % improvements

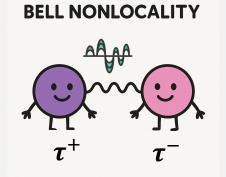
Summary



- $pp \to Z \to \tau \bar{\tau}$ is an excellent channel for Quantum Entanglement and Bell Nonlocality study:
 - More statistics than $t\bar{t}$ channels;
 - Good ν reconstruction can be achieved by using Diffusion + PET;
 - > 5σ has been obtained for entanglement and Bell nonlocality only using **Run2 data**;
 - Dr. Yulei Zhang proposed this analysis within the ATLAS Standard Model group and has already initiated a feasibility study using official ATLAS datasets.
- Thank to Vinicius Mikuni and Benjamin Nachman for their help in using OmniLearn.
- Special thanks to Tong Arthur Wu, Matthew Low and Tao Han for their detailed and expert guidance on the theory of this study.

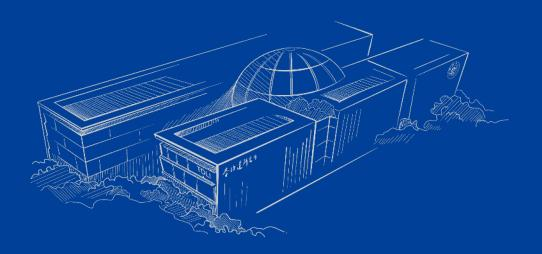








Thanks!



C and B calculation



• Consider a state ρ for a bipartite system with sub-systems i and j, it can be written as follows:

$$\rho = \frac{1}{4} \left(\mathbb{I}_2 \otimes \mathbb{I}_2 + \sum_i B_i^+ \sigma_i \otimes \mathbb{I}_2 + \sum_j B_j^- \mathbb{I}_2 \otimes \sigma_j + \sum_{ij} C_{ij} \sigma_i \otimes \sigma_j \right)^{[1]}$$



Here, $B_{i,j}^{\pm}$ characterizes the net polarization of the τ^{\pm} , C_{ij} describers the spin correlations, and i,j=1,2,3. Once ρ is reconstructed, we can calculate the concurrence C and Bell variable B.

- The definition of the C and B are as follow:
 - $C = \max(0, \lambda_1 \lambda_2 \lambda_3 \lambda_4)$, $\lambda_i = \sqrt{r_i}$, r_i is the eigenvalue, in descending magnitude of the matrix $\rho(\sigma_2 \otimes \sigma_2)$ $\rho^*(\sigma_2 \otimes \sigma_2)$; C > 0 for entanglement state; [2]
 - $B = \max(\sqrt{2}|C_{ii} \pm C_{jj}| 2); B > 0$ for Bell nonlocality; [3]

^[1] Pairs of two-level systems;

^[2] Entanglement of Formation of an Arbitrary State of Two Qubits;

^[3] Quantum tops at the LHC: from entanglement to Bell inequalities;

Trigger



- Di-tau trigger $(\pi\pi, \pi\rho, \rho\rho)$:
 - Leading τ : $p_T > 35 GeV$;
 - Sub-leading τ : $p_T > 25 GeV$;

(HLT tau35 medium1 tracktwo tau25 medium1 tracktwo L1TAU20IM 2TAU12IM)

- Moun+Tau trigger $(\pi\mu, \rho\mu)$:
 - τ : $p_T > 25 GeV$;
 - μ : $p_T > 14 GeV$;
 - (Or μ : $p_T > 25 GeV$)

(HLT mu14 tau25 medium1 tracktwo | | HLT mu26 ivarmedium)

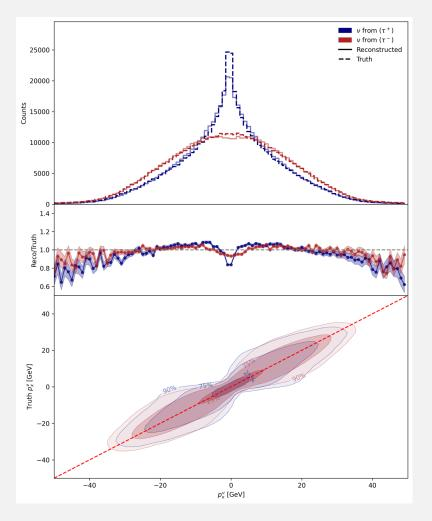
- Electron+Tau trigger $(\pi\mu, \rho\mu)$:
 - τ : $p_T > 25 GeV$;
 - $e: p_T > 17 GeV$;
 - (Or $e: p_T > 26 GeV$)

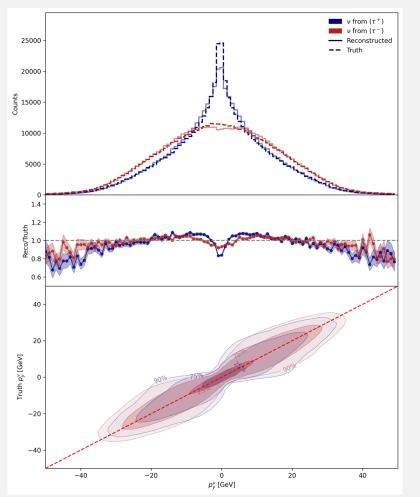
(HLT e17 lhmedium nod0 ivarloose tau25 medium1 tracktwo||HLT e26 lhtight nod0 ivarloose)

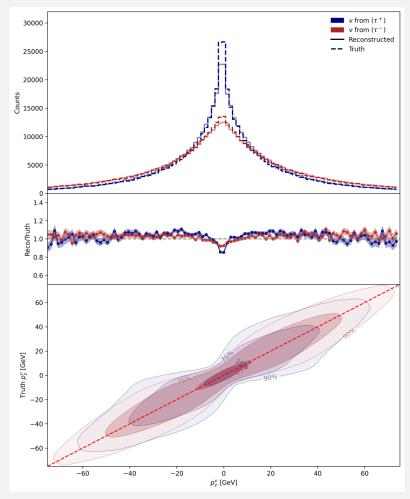
• Neutrino Reconstruction - $l\pi$



• We have achieved excellent reconstruction results for the three-momentum of ν .



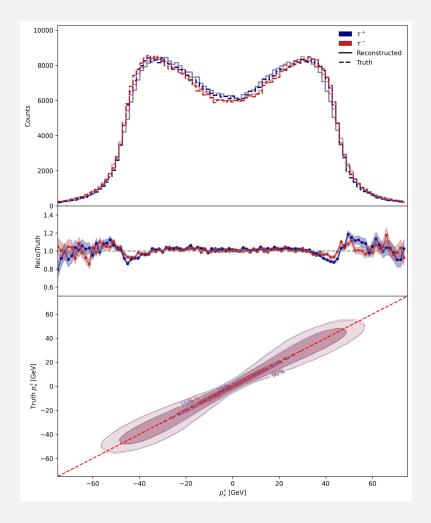


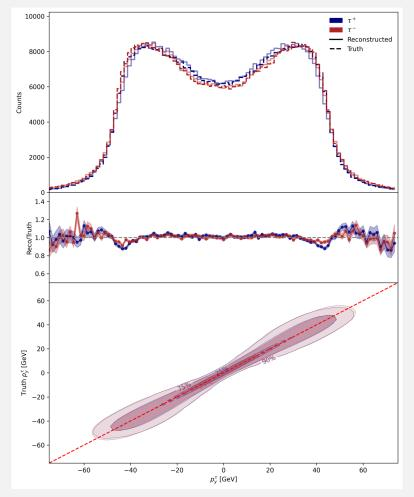


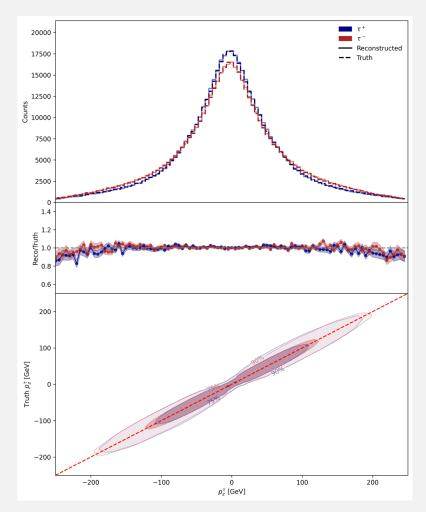
• Neutrino Reconstruction - $l\pi$



• We have achieved excellent reconstruction results for the three-momentum of τ .



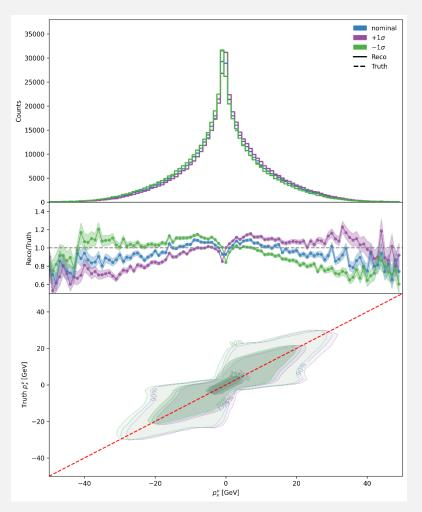


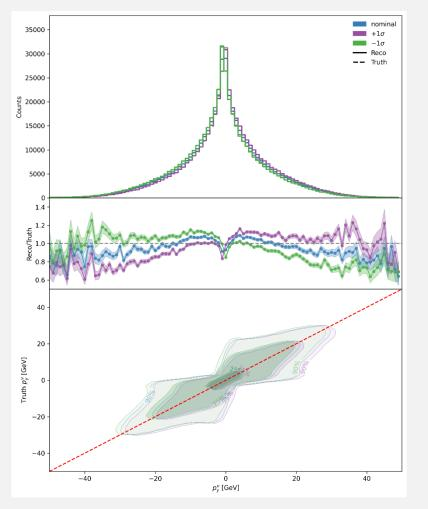


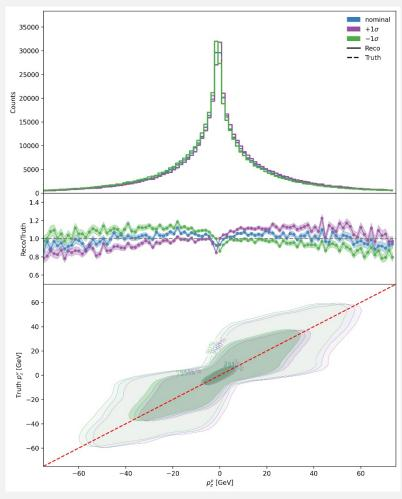
Neutrino Reconstruction - Systematics



• The stability of the **output** of the network is evaluated by **shifting the output by** $\pm \sigma$;







Systematics



		SR Only		SR & Trigger			
	ho ho	μho	Combined	ho ho	μho	Combined	
All Systematics	29.81%	$\boldsymbol{29.76\%}$	$\boldsymbol{31.29\%}$	31.00%	$\boldsymbol{29.82\%}$	$\boldsymbol{31.35\%}$	
MC Statistics	29.31%	29.56%	30.05%	28.93%	29.55%	28.66%	
Luminosity	0.12%	0.08%	0.90%	7.73%	0.74%	6.10%	
Background Cross-Section	3.39%	0.07%	2.01%	1.51%	0.05%	1.06%	
Signal Cross-Section	0.23%	0.23%	1.71%	3.12%	0.52%	2.41%	
Tau Energy Scale	1.47%	2.50%	2.12%	1.20%	0.89%	1.47%	
Jet Enery Scale	1.67%	1.50%	4.49%	2.41%	1.72%	8.05%	
Soft MET (p_x, p_y)	3.66%	1.90%	6.57%	6.68%	3.42%	7.11%	
ν Sampling	0.02%	0.02%	0.03%	0.06%	0.03%	0.07%	

Training and Evaluation details



- The dataset is split into training (80%), validation (20%) subsets;
- Training is conducted on 16 NVIDIA A100 GPUs using Horovod on the Perlmutter Supercomputer;
- The learning rate begins at 1.2×10^{-4} , following a warm-up phase and cosine decay schedule.
- We employ the Lion optimizer and implement an early stopping strategy;
- During evaluation, we generate **10 candidates** for each event and **randomly select one** as the final result to mitigate any bias introduced by the generation model;
- For DDIM, the parameters are set as $N_{steps} = 100$, $\eta = 1.0$;



Training Times



• Below is a table presenting the **training times**:

Subchannel	Time per epoch/s	Number of training epochs
$\pi\pi$	31	613
$e\pi$	30	1000
$\mu\pi$	39	1000
πho	11	381
e ho	9	488
μho	8	534
ho ho	11	900

For evaluation, approximately 15 minutes are required to process around 470k events,
 each with 10 candidate outputs.

• Neutrino Reconstruction – $l\pi$



• We randomly designated 10% of background jets as τ for fake estimation for $l\pi$ subchannel;

The plots demonstrate that the
network accurately reproduces the
ττ system mass peak, rather than
simply clustering all physical
processes around 90 GeV.

